Chemistry and Materials Research
ISSN 2224- 3224 (Print) ISSN 2225- 0956 (Online)
Vol.11 No.10, 2019

Studying Structural Properties and Fourier Transformation Infrared Spectrum of Sb Doped SnO_2 Powders Prepared by Solid State Reaction

Samia Haj Najeeb[1]* Ahmad Khdro[2] Talal khalas[3]
1.MSc Student, Department of Physics, Faculty of science, Tishreen University, Syria
2.Professor, Department of Physics, Faculty of science, Tishreen University, Syria
3.Assistant Professor, Department of Physics, Faculty of science, Tishreen University, Syria

Abstract
Sb doped tin oxide transparent conducting powder were prepared by solid state reaction method. Structural properties of the samples were investigated as a function of various Sb-doping levels (x=0.00-0.01-0.02-0.04-0.06). The results of x-ray diffraction have shown that the samples are polycrystalline structure in tetragonal phase with preferential orientations along the (110) and (101) planes.the relative intensities, distance between crystalline planes (d), crystallite size (D), dislocation density (δ) and lattice parameters (a), (c) were determined. Infrared Spectroscopy have been studied by Infrared Spectrometer Device.
Keywords: powder, Antimony doped Tin Oxide, solid state reaction, Structural properties, Infrared Spectroscopy.
DOI: 10.7176/CMR/11-10-03
Publication date: December 31st 2019

1. Introduction

Nano-crystals of semiconductor metal oxides have attracted a great interest due to their intriguing properties, which are different from those of their corresponding bulk state [1]. Tin dioxide SnO2 has achieved special attention among the metal oxides, because of its wide band gap (3.6eV), optical transparency and high carrier density, thermal and chemical stabilities [2 , 3].

Because of its unique electronic, optical, electrochemical and catalytical properties, it has been widely used in flat panel displays, transparent conducting electrodes , solar cells , gas sensors and rechargeable Li – ion batteries , etc [4].

It crystallizes in the tetragonal rutile structure with space group P42/mnm . the lattice parameters a=b= 4.738 Å and c = 3.187 Å [5].

Its unit cell contains two tin and four oxygen atoms as is shown in figure (1) . The tin atom is at the center of six oxygen atoms placed at the corners of a regular octahedron. Every oxygen atom is surrounded by three tin atoms at the corners of an equilateral triangle [6].

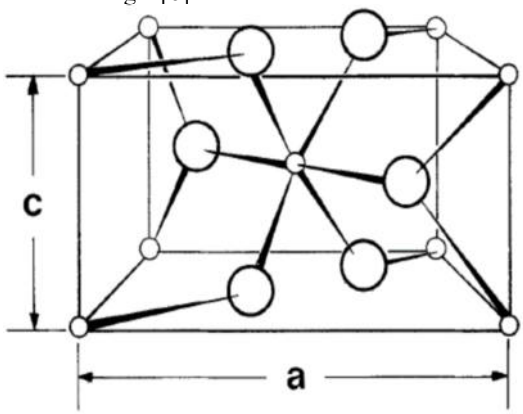

Fig (1) : Unit cell of the crystal structure of SnO_2. Large circles indicate oxygen atoms and the small circles indicate tin atoms.

The aim of this paper is preparing a doped metal oxide $Sn_{1-x}Sb_xO_2$ and characterizing by X-ray and FTIR to study the structural properties.

2 . Experimental Method

$Sn_{1-x}Sb_xO_2$ powders (x = 0.00 - 0.01 - 0.02 - 0.04 - 0.06) were prepared by a solid state reaction method. were accurately weighed in required proportions and were mixed and ground thoroughly using an Agate mortar and pestle to convert to very fine powders.

The grinding of the mixtures was carried out for 3 hours for all the powder samples. The ground powder

samples were firing at 700°C for 3 hours.

3 . Results and discussions

3.1 Structural properties

The X-ray diffraction patterns of undoped and Sb doped SnO2 powders prepared with various Sb concentration 0 wt%, 1 wt%, 2 wt%, 4 wt% and 6 wt% are shown in Figure (2) . The XRD reveals that all samples are having polycrystalline nature with tetragonal structure and peaks correspond to (110) , (101) , (200) , (111) , (210) , (211) , (220) , (002) , (310) , (112) , (301) , (202) and (321) planes. The preferred orientation is (110) for pure and Sb doped SnO_2 powders at 1 and 4 wt% doping , but for 2 and 6 wt% doping the preferred orientation change to (101) plane .

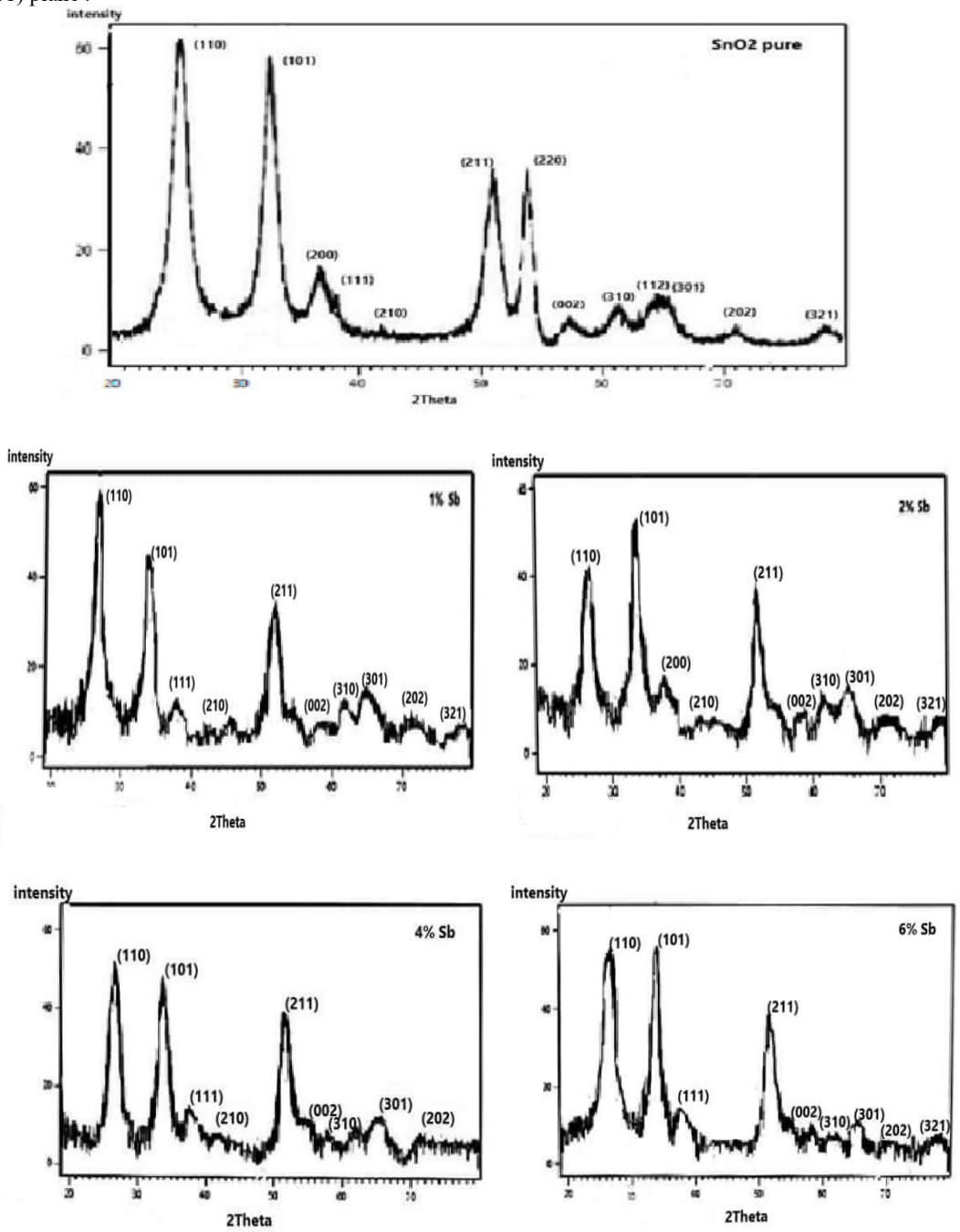

Fig (2): XRD results of pure SnO_2, 1 wt% Sb doped SnO_2, 2 wt% S doped SnO_2, 4 wt% Sb doped SnO_2, 6 wt% Sb doped SnO_2.

Table (1) shows results of structural values of undoped SnO_2 sample.

Table (1)

samples	2θ (deg)	)hkl(	d (Å)	Rel. int. [%]	β (deg)	D (nm)	Average D(nm)	δ 10^{15}line/m^2	Lattice const.	
									a(Å)	c(Å)
SnO_2 pure	26.62	(110)	3.348	100	1.392	6.128	11.877	26.628	4.733	3.185
	33.99	(101)	2.637	87	1.391	6.240		25.680		
	37.95	(200)	2.370	25	0.886	9.908		10.187		
	38.96	(111)	2.311	7	0.440	20.012		2.497		
	42.62	(210)	2.121	4	0.510	17.471		3.276		
	51.87	(211)	1.762	58	1.265	7.297		18.783		
	54.75	(220)	1.676	58	0.506	18.473		2.930		
	57.87	(002)	1.593	11	1.012	9.372		11.385		
	61.99	(310)	1.497	14	1.341	7.221		19.180		
	64.84	(112)	1.437	17	1.898	5.180		37.261		
	65.96	(301)	1.416	15	0.632	15.656		4.080		
	71.25	(202)	1.323	7	1.645	6.207		25.955		
	78.30	(321)	1.221	10	0.424	25.240		1.570		

Table (2) shows results of structural values of Sb doped SnO_2 samples (x=0.01-0.02).

Table (2)

samples	2θ (deg)	)hkl(	d (Å)	Rel. int. [%]	β (deg)	D (nm)	Average D(nm)	δ 10^{15} line/m^2	Lattice const.	
									a(Å)	c(Å)
SnO_2:Sb (1 wt%)	26.62	(110)	3.345	100	1.15	7.414	5.971	18.191	4.731	3.161
	33.89	(101)	2.642	72	1.45	5.982		27.944		
	38.15	(111)	2.357	15	2.01	4.367		52.415		
	42.51	(210)	2.124	4	0.82	10.857		8.483		
	51.98	(211)	1.757	55	1.49	6.195		26.054		
	58.32	(002)	1.580	8	1.85	5.135		37.909		
	62.23	(310)	1.490	11	1.79	5.414		34.111		
	65.36	(301)	1.426	13	2.42	4.073		60.264		
	71.86	(202)	1.312	6	1.95	5.254		36.213		
	78.25	(321)	1.220	10	2.13	5.021		39.659		
SnO_2:Sb (2 wt%)	26.85	(110)	3.317	80	1.85	4.611	5.741	47.032	4.692	3.167
	33.94	(101)	2.639	100	1.15	7.543		17.573		
	37.96	(200)	2.368	12	1.56	5.624		31.609		
	43.25	(210)	2.090	6	2.12	4.210		56.415		
	52.16	(211)	1.752	68	1.25	7.390		18.309		
	58.2	(002)	1.583	9	1.46	6.504		23.638		
	61.95	(310)	1.496	7	1.77	5.467		33.452		
	65.78	(301)	1.418	13	1.95	5.067		38.945		
	71.35	(202)	1.320	4	2.22	4.600		47.238		
	78.99	(321)	1.211	9	1.68	6.400		24.412		

Table (3) shows results of structural values of Sb doped SnO_2 samples (x=0.04-0.06).

Table (3)

samples	2θ (deg)	)hkl(	d (Å)	Rel. int. [%]	β (deg)	D (nm)	Average D(nm)	δ 10^{15} line/m^2	Lattice const.	
									a(Å)	c(Å)
SnO_2:Sb (4 wt%)	26.63	(110)	3.344	100	1.92	4.440	6.532	50.705	4.730	3.129
	34.12	(101)	2.625	80	1.83	4.742		44.456		
	38.1	(111)	2.360	10	1.52	5.775		29.983		
	42.22	(210)	2.138	5	1.35	6.588		23.038		
	52.27	(211)	1.748	69	1.75	5.281		35.852		
	58.98	(002)	1.564	7	0.98	9.726		10.569		
	61.85	(310)	1.498	9	1.15	8.410		14.136		
	65.34	(301)	1.427	15	2.1	4.693		45.390		
	71.52	(202)	1.318	4	1.12	9.129		11.997		
SnO_2:Sb (6 wt%)	26.25	(110)	3.392	94	1.52	5.605	5.186	31.828	4.797	3.150
	33.88	(101)	2.643	100	1.75	4.956		40.706		
	38.02	(111)	2.364	15	1.86	4.718		44.919		
	52.21	(211)	1.750	48	1.96	4.714		44.995		
	58.56	(002)	1.575	7	1.62	5.872		29.001		
	61.84	(310)	1.499	4	2.15	4.498		49.414		
	65.15	(301)	1.430	16	1.65	5.967		28.081		
	70.85	(202)	1.328	6	1.82	5.594		31.948		
	78.15	(321)	1.222	10	2.25	4.750		44.316		

The relative intensities of undoped and Sb doped SnO_2 powders are calculated. The distance between crystalline planes values (d) are calculated by using following relation:

$$2d.\sin\theta = n\lambda \qquad (1)$$

Where d is distance between crystalline planes (A), θ is the Bragg angle, λ is the wavelength of X-rays (λ=1.54056 Å).

The crystallite size is calculated from Scherrer's equation [7]:

$$D = \frac{0.94\lambda}{\beta cos\theta} \qquad (2)$$

Where, D is the crystallite size, λ is the wavelength of X-ray, β is full width at half maximum (FWHM) intensity in radians and θ is Braggs's angle.

The dislocation density is defined as the length of dislocation lines per unit volume and calculated by following equation [8]:

$$\delta = \frac{1}{D^2} \qquad (3)$$

The lattice constants a and c for tetragonal phase structure are determined by the relation [9]:

$$\frac{1}{d^2} = \frac{h^2+k^2}{a^2} + \frac{l^2}{c^2} \qquad (4)$$

Where d and (hkl) are distance between crystalline planes and Miller indices, respectively.

The calculated lattice constants a, c values are given in table 1,2,3. It was seen that a, c and c/a match well with JCPDS data (a=b= 4.737 Å and c= 3.185 Å).

The change in peak intensities is basically due to the replacement of Sn^{4+} ions with Sb^{5+} ions in the lattice of the SnO2.

Figure (3) represents variation of the average grain size with different concentrations of Sb doped SnO2 powdres.

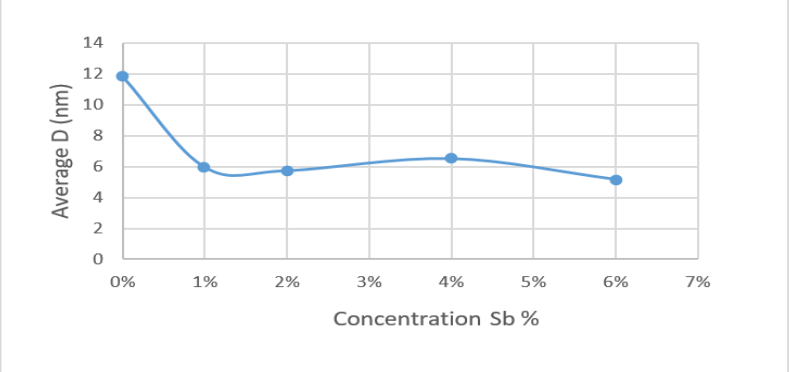

We observed that the crystallite size decrease with increasing of the antimony ion content . this is due to the fact that the Sb^{5+} radius (0.62 Å) is smaller than the Sn^{4+} (0.69 Å) , and the replacement process which causes shrinkage of the lattice [10 , 11] .

4 .FT/IR analysis:

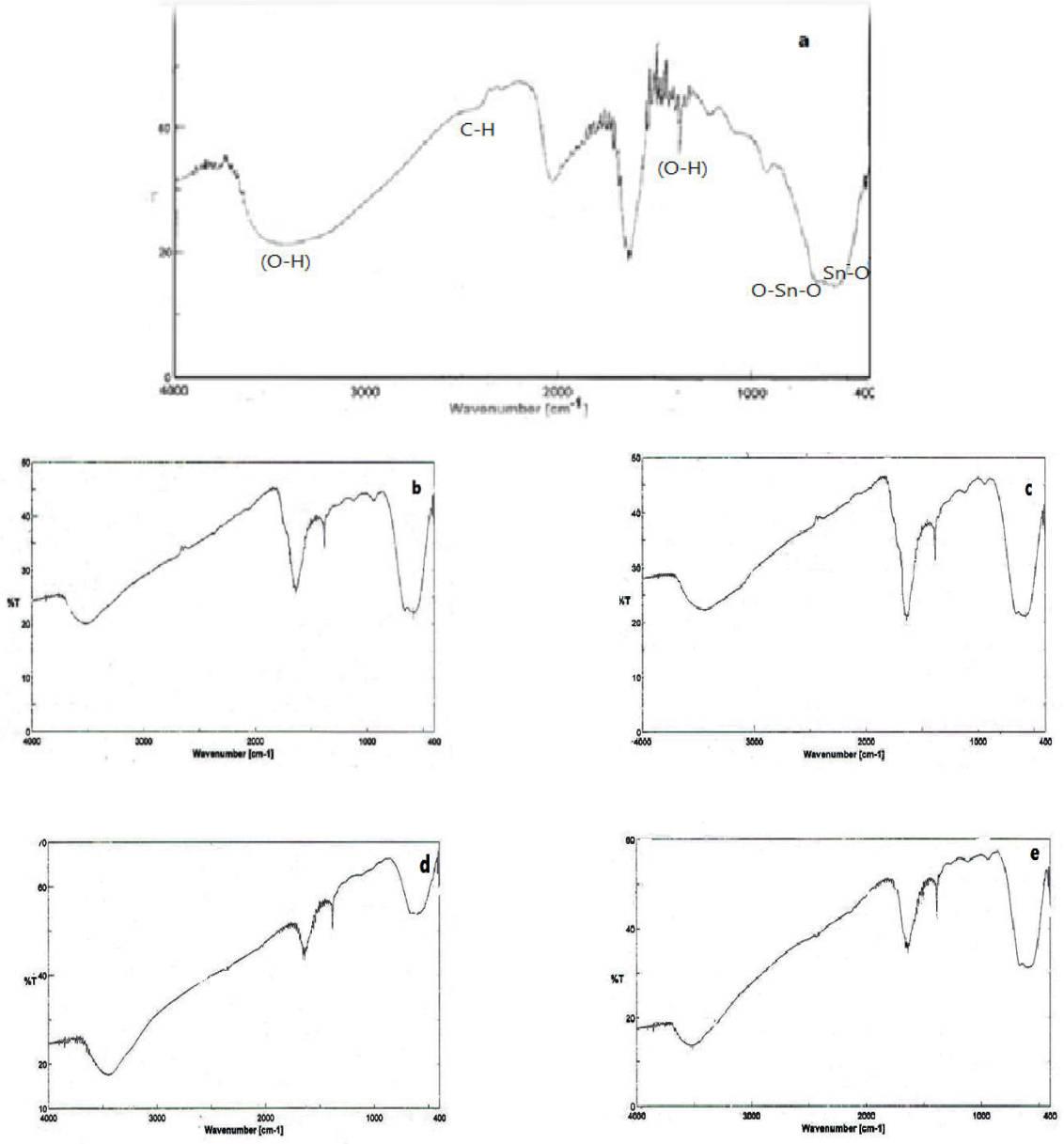

Fig (4): FTIR analysis of pure and Sb doped SnO_2 powder :(a) pure (b) 1 wt% Sb doped SnO_2, (c) 2 wt% Sb doped SnO_2, (d) 4 wt% Sb doped SnO_2, (e) 6 wt% Sb doped SnO_2

FTIR is a technique used to obtain information regarding chemical bonding and functional groups in a material. In the transmission mode, it is quite useful to predict the presence of certain functional groups which are adsorbed at certain frequencies; thus, it reveals the structure of the material. The band positions and numbers of absorption peaks depend on the crystalline structure, chemical composition, and also on morphology [12]. To investigate chemical groups on the surface of sintered samples, an FTIR analysis was carried out at room temperature over the wave number range of 400– 4000 cm^{-1}. There are several bands appearing in the wave number range 400–4000 cm^{-1}. The broad absorption band at 3423 cm^{-1}, the peaks at 2977 cm^{-1}, and 1630 cm^{-1} are assigned to the vibration of hydroxyl group due to the absorbed/adsorbed water and show a stretching vibrational mode of O–H group [13]. Absorption peaks observed around 2380 cm^{-1} belong to the stretching vibrations of C–H bonds

that could be due to the adsorption and interaction of atmospheric carbon dioxide with water during the firing process [14].the main IR features of SnO_2 appear at 468 and 609 cm^{-1} . which assign to O – Sn – O and Sn – O stretching vibration , respectively [15].

The changing in the shapes and positions of absorption peaks indicates to presence of stretching modes, which are, give an indication of successful doping Sb to tin oxide nanoparticles [16].

5. Conclusion

This paper presents a study of structural properties of Sb doped SnO_2 powders prepared by solid state reaction method. X-ray diffraction patterns confirm that the samples have polycrystalline nature with tetragonal structure and show presence (110)، (101)، (200)، (111)، (210)، (211)، (220)، (002)، (310)، (112)، (301)، (202) and (321) planes in pure tin oxide sample. The SnO_2 have preferred orientation along (110) for all samples , but for (0.02 , 0.06) doping levels the preferred orientation change to (101) plane . The average of crystallite size is within the range [11.877- 5.186 nm] for all samples. It was defined that the lattice constants a, c for all the samples, were almost identical with JCPDS values, and the ratio c/a remained constant with increasing Sb dopant concentration. FTIR analysis revealed that the Sb doping manifests itself by a shift in Sn–O absorption peaks positions.

REFERANCE:

[1] - Ashock.D.Bhagwat , Sachin.S.Sawant , Balaprasad G.Ankamwar , Chandrashekhar M.Mahajan . (2015) '' Synthesis of Nanostructured Tin Oxide SnO_2 powders and Thin films by Sol-gel method '', *J.Nano and Electronic*, Vol.7 , No.4, 04037 , (4pp) .

[2] - K. Subramanyama, N.Sreelekha a, G.Murali b, D.AmaranathaReddy c, R.P.Vijayalakshmi. (2014) "Structural,optical and magnetic properties of Cr doped SnO2 nanoparticles stabilized with polyethylene glycol", *PhysicaB454* , 86–92.

[3] - S.A.Wolf,D.D.Awschalom,R.A.Buhrman,J.M.Daughton,S.VonMolnar, M.L. Roukes, A.Y. Chtchelkanova, D.M.Treger. (2001)" Spintronics: A Spin- Based Electronics Vision for the Future"*Science*,294, 1488–1495.

[4] - C.Wang , J.Li , Y.Zhang , Y.Wei , J.Liu . (2010) , *J.Alloys Compd* .493 , 64-69 .

[5] - G.McCarthy , J.Wetton , *Powder Diffraction* 4 , (1989) 156 .

[6] - Jarzebski Z. & Marton J. (1976) "Physical Properties of SnO2 Materials", *Journal of the Electrochemical Society*, 199-205.

[7] - Mariappan R., Ponnuswamy V. & Suresh P. (2012) "Effect Of Doping Concentration On The Structural And Optical Properties Of Pure And Tin Doped Zinc Oxide Thin Films By Nebulizer Spray Pyrolysis (NSP) Technique", *Superlattices and Microstructures*, 52, 500-513.

[8] - Turgut G., Keskenler E. F., Aydin S.; Sonmez E., Dogan S., Duzgun B. & Ertugrul M. (2013), "Effect Of Nb Doping On Structural, Electrical And Optical Properties Of Spray Deposited SnO2 Thin Films", *Super lattices and Microstructures*, 56, 107-116.

[9] - Gurakar S., Serin T & Serin N. (2014) "Electrical And Microstructural Properties Of (Cu, Al, In)-Doped SnO2 Films Deposited By Spray Pyrolysis", *Advanced Materials Letters*, 5(6), 309-314.

[10] - N.B.IbrahimM.H.AbdiM.H.AbdullahH.Baqiah. (2013) " Structural and optical characterisation of undoped and chromium doped tin oxide prepared by sol–gel method ", *App. Surf. Sci*. 271, 260-264.

[11]- L. Zhang, S. Ge, Y. Zuo, J. Wang, J. Qi, (2010) "Ferromagnetic properties in undoped and Cr-doped SnO2 nanowires", *Scripta Materialia* 63, 953–956.

[12] - Ashokkumar.M,et al, (2014) ," $Zn0._{96-x}Cu_{0.04}Fe_xO(0 \leqslant x \leqslant 0.04)$ alloys – Optical and structural studies), *Superlattices and Microstructures*, 69, 53-64.

[13] - Faisal.M, et al, (2015), "SnO_2 doped ZnO nanostructures for highly efficient photocatalyst", *Journal of Molecular catalysis A: chemical*, 39, 19-25.

[14] - Gnanam.S, Rajendran.V, (2010)," Preparation of Cd-doped SnO_2 nanoparticles by sol–gel route and their optical properties", *Journal of Sol-Gel Science and Technology*, 56, 128–133.

[15] – Kuantama E, Han DW, Sung YM, Song JE, Han CH. *Thin Solid Films*. (2009); 517:4211-4.

[16] - S.Blessi, M. Maria Lumina Sonia, S.Vijayalakshmi and S.Pauline. (2014) " Preparation and characterization of SnO2 nanoparticles by hydrothermal method", *Int. J. of ChemTech Res* , 6(3), 2153-2155.